THE JOURNAL OF BIOLOGICAL CHEMISTRY
Vol. 276, No. 24, Issue of June 15, pp. 21489–21499, 2001

Printed in U.S.A.

Glucagon-like Peptide (GLP)-2 Action in the Murine Central Nervous System Is Enhanced by Elimination of GLP-1 Receptor Signaling*

Received for publication, October 13, 2000, and in revised form, March 19, 2001
Published, JBC Papers in Press, March 21, 2001, DOI 10.1074/jbc.M009382200

Julie Lovshin‡§, Jennifer Estall‡, Bernardo Yusta‡, Theodore J. Brown¶, and Daniel J. Drucker‡‖

From the ‡Department of Medicine, Banting and Best Diabetes Centre, Toronto General Hospital, and the ¶Division of Reproductive Science, Samuel Lunenfeld Research Institute, Mount Sinai Hospital, Toronto, Ontario M5G 1Y5, and the University of Toronto, Toronto, Ontario M5G 2C4, Canada

Glucagon-like peptide-2 (GLP-2) regulates energy homeostasis via effects on nutrient absorption and maintenance of gut mucosal epithelial integrity. The biological actions of GLP-2 in the central nervous system (CNS) remain poorly understood. We studied the sites of endogenous GLP-2 receptor (GLP-2R) expression, the localization of transgenic LacZ expression under the control of the mouse GLP-2R promoter, and the actions of GLP-2 in the murine CNS. GLP-2R expression was detected in multiple extrahypothalamic regions of the mouse and rat CNS, including cell groups in the cerebellum, medulla, amygdala, hippocampus, dentate gyrus, pons, cerebral cortex, and pituitary. A 1.5-kilobase fragment of the mouse GLP-2R promoter directed LacZ expression to the gastrointestinal tract and CNS regions in the mouse that exhibited endogenous GLP-2R expression, including the cerebellum, amygdala, hippocampus, and dentate gyrus. Intracerebroventricular injection of GLP-2 significantly inhibited food intake during dark-phase feeding in wild-type mice. Disruption of glucagon-like peptide-1 receptor (GLP-1R) signaling with the antagonist exendin-(9–39) in wild-type mice or genetically in GLP-1R$^{-/-}$ mice significantly potentiated the anorectic actions of GLP-2. These findings illustrate that CNS GLP-2R expression is not restricted to hypothalamic nuclei and demonstrate that the anorectic effects of GLP-2 are transient and modulated by the presence or absence of GLP-1R signaling *in vivo*.

The glucagon-like peptides are liberated in the gut and central nervous system via tissue-specific post-translational processing of a common proglucagon precursor (1). Glucagon-like peptide-1 (GLP-1) [1] and GLP-2 are secreted from the gut following nutrient ingestion and regulate nutrient absorption and energy homeostasis (2, 3). The actions of GLP-1 include regulation of gastric emptying, gastric acid secretion, inhibition of food intake and glucagon secretion, and stimulation of glucose-dependent insulin secretion and insulin biosynthesis (2–5). GLP-1 also promotes expansion of islet mass via stimulation of β-cell proliferation and induction of islet neogenesis via increased ductal *Pdx-1* expression (6, 7). Taken together, these actions maintain euglycemia, hence enhancing GLP-1 action represents a potential strategy for the treatment of diabetes mellitus.

GLP-2 exhibits trophic properties in the small and large bowel characterized by expansion of the mucosal epithelium via stimulation of crypt cell proliferation and inhibition of apoptosis (8–10). GLP-2 also regulates gastric motility, gastric acid release, intestinal permeability, and intestinal hexose transport, actions independent of its effects on epithelial growth (11–14). The intestinotrophic and cytoprotective properties of GLP-2 have been evaluated in the setting of acute intestinal injury, where GLP-2 administration inhibits apoptosis and reduces the severity of mucosal damage in both the small and large intestine (15–18).

In the central nervous system (CNS), the glucagon-like peptides are synthesized predominantly in the caudal brainstem and, to a lesser extent, in the hypothalamus (19–21). The GLP-1 receptor (GLP-1R) is expressed more widely throughout the CNS (22, 23), and GLP-1 has been shown to regulate appetite, hypothalamic pituitary function, and the central response to aversive stimulation (24–29). Peripheral administration of GLP-1 or the lizard GLP-1 analog exendin-4 also reduces food intake and body weight (30, 31), suggesting that gut-derived GLP-1 provides signals that influence feeding behavior either directly to the brain or indirectly, likely via vagal afferents.

In contrast to the increasing number of studies describing CNS actions of GLP-1, much less is known about the potential function(s) of GLP-2 in the brain. Experiments using rat hypothalamic and pituitary membranes demonstrated GLP-2-mediated activation of adenylate cyclase (32). Consistent with these findings, the actions of GLP-2 were subsequently shown to be transduced in a cAMP-dependent manner via a recently cloned GLP-2 receptor (GLP-2R) isolated from hypothalamic and intestinal cDNA libraries (33). The GLP-2R is expressed in a highly tissue-specific manner predominantly in gut endocrine cells and in the brain (33, 34). In comparison with GLP-1, little

* This work was supported in part by operating grants from the Canadian Institutes of Health Research and the Ontario Research and Development Challenge Fund. The costs of publication of this article were defrayed in part by the payment of page charges. This article must therefore be hereby marked "*advertisement*" in accordance with 18 U.S.C. Section 1734 solely to indicate this fact.

The nucleotide sequence(s) reported in this paper has been submitted to the GenBank™/EBI Data Bank with accession number(s) AF338223 and AF338224.

§ Recipient of a doctoral research award from the Canadian Institutes of Health Research.

‖ Canadian Institutes of Health Research Senior Scientist. To whom correspondence should be addressed: Banting and Best Diabetes Centre, Toronto General Hospital, 101 College St., CCRW3–845, Toronto, Ontario M5G 2C4, Canada. Tel.: 416-340-4125; Fax: 416-978-4108; E-mail: d.drucker@utoronto.ca.

[1] The abbreviations used are: GLP-1 and GLP-2, glucagon-like peptide-1 and -2, respectively; hGLP-2, human GLP-2; GLP-1R and GLP-2R, GLP-1 and GLP-2 receptors, respectively; CNS, central nervous system; RT-PCR, reverse transcription-polymerase chain reaction; RACE, rapid amplification of cDNA ends; bp, base pair(s); kb, kilobase(s); PBS, phosphate-buffered saline; X-gal, 5-bromo-4-chloro-3-indolyl β-D-galactopyranoside; BHK, Baby hamster kidney.

is known about either the expression or function of the GLP-2R in different regions of the CNS.

Both GLP-1- and GLP-2-immunoreactive fiber tracts project from the brainstem to multiple CNS regions, including the hypothalamus, thalamus, cortex, and pituitary (21, 35). Intracerebroventricular infusion of GLP-2 in rats inhibits food intake (35), similar to results obtained following intracerebroventricular infusion of GLP-1 (24, 36). Unexpectedly, the anorectic effects of GLP-2 in rats are completely inhibited by the GLP-1R antagonist exendin-(9–39) (35). These findings imply that CNS GLP-2 may exert its effects via the GLP-1R to inhibit food intake, or alternatively, exendin-(9–39) may also function as a CNS GLP-2R antagonist. Furthermore, although expression of the rat GLP-2R was reported to be restricted to the dorsomedial nucleus of the hypothalamus by *in situ* hybridization (35), other studies have reported a more widespread distribution of GLP-2R mRNA transcripts in various regions of the rat CNS (37). To understand the biological function and mechanisms regulating control of GLP-2R expression in the brain, we have now studied GLP-2R expression and GLP-2 action in the rodent CNS using a combination of immunohistochemical, reverse transcription-polymerase chain reaction (RT-PCR), transgenic, and cell-based analyses.

EXPERIMENTAL PROCEDURES

All animal experiments were approved and carried out strictly in accordance with the Canadian Council on Animal Care guidelines and the Animal Care Committee at the Toronto General Hospital, University Health Network (Toronto, Ontario, Canada). Animals were allowed to acclimatize to the animal care facilities for at least 1 week prior to any experimental procedure.

Characterization of GLP-2R Sequences and Transgene Construction—A genomic clone containing the 5′-flanking, 5′-untranslated, and coding regions of the murine GLP-2R gene was isolated from a 129SVJ mouse genomic library. To identify additional GLP-2R nucleotide sequences 5′ to the translation start site (33), the 5′-end of the rat GLP-2R cDNA was generated and characterized using adaptor-modified complementary DNA from rat brain (CLONTECH, Palo Alto, CA) in 5′-rapid amplification of cDNA ends (RACE) experiments. Separately, a 1516-base pair (bp) fragment of the mouse GLP-2R gene was subcloned from the mouse genomic library (Incyte Genomics, St. Louis, MO), sequenced, and ligated immediately 5′ to a cDNA encoding LacZ with a nuclear localization signal (a gift from A. Nagy). The GLP-2R promoter-*lacZ* transgene was gel-purified and used for generation of transgenic mice. In total, eight founder animals were identified by Southern blotting and PCR analysis and mated with non-transgenic mice to determine germ-line transmission of the transgene. Three transgenic founder mice (designated lines 2–4) exhibited germ-line transmission and were used to generate lines for further analysis of transgene expression.

CNS Tissue Dissections—Male Harlan Sprague-Dawley rats (300–500 g) or GLP-2R promoter-*lacZ* transgenic mice were killed by CO_2 inhalation and quickly decapitated. The brains were rapidly removed and placed ventral side up on a chilled glass plate. The pituitary glands were also removed and frozen in liquid nitrogen. The amygdala, cerebral cortex, cerebellum, pons/midbrain, and medulla were dissected and frozen in liquid nitrogen. The amygdala was dissected by first producing a 3-mm thick coronal section by making a coronal cut at the optic chiasm and at the posterior edge of the mamillary bodies. A cut connecting the rhinal fissures formed the dorsal boundary of the amygdaloid block, and cuts made continuous with the lateral ventricles to the lateral hypothalamic sulci formed the medial boundaries of the amygdaloid blocks. The cerebral cortex was also taken from this coronal section and consisted primarily of parietal and frontal cortices. The cerebellum was removed, and a coronal cut was made at the posterior edge of the pons. The neural tissue posterior to this cut comprised the medulla, which also contained the anterior-most portion of the spinal cord. The midbrain block, which also included the pons, extended from the posterior edge of the mamillary bodies to the posterior edge of the pons, with the cerebellar and cerebral cortices, hippocampus, and amygdala removed.

RNA Isolation and RT-PCR Analyses—Total RNA was isolated from CNS tissues using Trizol™ reagent (Life Technologies, Inc., Toronto) and from peripheral tissues using a modified guanidinium thiocyanate procedure (38) and dissolved in ribonuclease-free water. RNA integrity was assessed on a 1% (w/v) agarose gel containing formaldehyde and visualized on a UV transilluminator (Fisher, Montreal, Quebec, Canada) using ethidium bromide staining. For RT-PCR experiments, RNA samples were treated with DNase I (Life Technologies, Inc.), primed with random hexamers (Life Technologies, Inc.), and reverse-transcribed with Superscript™ II reverse transcriptase (Life Technologies, Inc.). To control for contamination, reactions were also carried out in the absence of Superscript™. Following first-strand cDNA synthesis, samples were treated with ribonuclease H (MBI Fermentas, Vilnius, Lithuania) to remove RNA. For subsequent PCR amplification, first-strand cDNA was used as template. Oligonucleotide primer pairs, annealing temperature, and cycle number for PCR amplification were as follows. For the rat GLP-2R, 5′-TTGTGAACGGGCGCCAGGAGA-3′ and 5′-GATCTCACTCTCTTCCAGAATCTC-3′ were annealed at 65 °C for 40 cycles; for the mouse GLP-2R, 5′-CTGCTGGTTTCCATCAAGCAA-3′ and 5′-TAGATCTCACTCTCTTCCAGA-3′ were annealed at 65 °C for 30 cycles; for rat glyceraldehyde-3-phosphate dehydrogenase, 5′-TCCACCACCCTGTTGCTGTAG-3′ and 5′-GACCACAGTCCATGACATCACT-3′ were annealed at 60 °C for 30 cycles; and for the GLP-2R-*lacZ* transgene, 5′-CGCTGATTTGTGTAGTCGGTT-3′ and 5′-CTTATTCGCCTTGCAGCACAT-3′ were annealed at 63 °C for 40 cycles. The expected PCR product for the mouse and rat GLP-2R cDNAs is ~1.6 kilobases (kb), corresponding to the full-length GLP-2R (33, 34). The predicted *lacZ* PCR product is ~580 bp; and for rat glyceraldehyde-3-phosphate dehydrogenase, the expected PCR product is ~450 bp. To control for nonspecific amplification, PCR reactions were also carried out in the absence of first-strand cDNA. Following amplification, PCR products were separated by gel electrophoresis; transferred onto a nylon membrane (GeneScreen, Life Technologies, Inc.); and hybridized with 1) a ^{32}P-labeled internal cDNA probe for the rat GLP-2R (33, 34), 2) a ^{32}P-labeled internal *lacZ* oligonucleotide (5′-TCAGGAAGATCGCACTCCAGC-3′), or 3) a ^{32}P-labeled internal cDNA probe for rat glyceraldehyde-3-phosphate dehydrogenase (39). Following hybridization, membranes were washed stringently, and hybridization signals were quantified on a Storm 840 PhosphorImager (Molecular Dynamics, Inc., Sunnyvale, CA) using ImageQuant™ software (Version 5.0, Molecular Dynamics, Inc.).

Immunocytochemistry—Rats or mice were deeply anesthetized following intraperitoneal injections of sodium pentobarbital. Following transcardial perfusion with 0.9% sodium chloride, animals were perfused with 4% neutral buffered Formalin for ~15 min. Brains were removed and post-fixed at room temperature for 4 h or overnight at 4 °C. Brains were then cryopreserved overnight in a 20% sucrose in phosphate-buffered saline (PBS) gradient at 4 °C, frozen slowly in dry ice vapor, and either stored at −80 °C or sectioned immediately at 10 μm on a cryostat. All sections were collected and thaw-mounted onto Superfrost Plus slides (Fisher). For detection of β-galactosidase-immunopositive cells, slides were incubated for 4 h at 37 °C in a 1:8000 dilution of polyclonal anti-β-galactosidase antiserum (ICN Pharmaceuticals Inc., Costa Mesa, CA). Polyclonal anti-GLP-2R antiserum (1:800) that recognizes the GLP-2R, but not the glucagon, glucose-dependent inhibitory polypeptide, and GLP-1 receptors (34), was a gift from NPS Allelix Corp. (Mississauga, Canada). To control for nonspecific immunopositivity, anti-GLP-2R antiserum was also preabsorbed overnight at 4 °C in the presence of recombinant GLP-2R immunogen (34), and immunocytochemistry studies were carried out with 1) anti-GLP-2R antiserum, 2) preimmune serum, 3) antibody diluent alone, or 4) preabsorbed anti-GLP-2R antiserum. All slides were counterstained in hematoxylin.

Histochemical Analysis—Brains were isolated from mice and placed in 2% paraformaldehyde and 0.2% glutaraldehyde in PBS fixative for 1 h at room temperature. Sixty minutes later, brains were rinsed in PBS and transferred to 4 °C in 15% sucrose in PBS solution for 4 h to overnight and subsequently to 30% sucrose in PBS solution for 4 h to overnight for cryopreservation. Brains were then frozen in dry ice vapor and stored at −80 °C. Tissues were sectioned at 10 μm in a −25–30 °C cryostat and subsequently thaw-mounted and stored at −80 °C. Prior to staining with 5-bromo-4-chloro-3-indolyl β-D-galactopyranoside (X-gal; Bioshop Canada, Burlington, Ontario), slides were slowly warmed to room temperature and rinsed in PBS. Slides were treated with X-gal solution overnight at 37 °C. Following treatment with X-gal solution, slides were rinsed in PBS, counterstained with eosin, and dehydrated in an ethanol series.

Microscopy—All slides were visualized and captured using a JVC video camera with a ½-inch chip device adapted (0.63 × c-mount) to a light microscope (Leica Ltd., Cambridge, United Kingdom). Magnification is reported as the objective magnification multiplied by the c-mount magnification multiplied by the electronic magnification (electronic

magnification was corrected for by dividing the diagonal of the image captured by the camera chip size).

Peptides—Recombinant h[Gly^2]GLP-2, a dipeptidyl peptidase IV-resistant GLP-2 analog (40, 41), was a gift from NPS Allelix Corp. Human GLP-1-(7–36)-NH_2, exendin-4, and exendin-(9–39) were purchased from California Peptide Research Inc. (Napa, CA). Forskolin and 3-isobutyl-1-methylxanthine were obtained from Sigma.

Analysis of GLP-2R Signaling in GLP-2R-transfected Baby Hamster Kidney (BHK) Cells—BHK fibroblast cells stably transfected with either the rat GLP-1R or GLP-2R were propagated as previously described (42), and the levels of intracellular cAMP were assayed following exposure to individual peptides in Dulbecco's modified Eagle's medium containing 100 μM 3-isobutyl-1-methylxanthine as reported (41, 42). Cells were incubated for 5 min with exendin-(9–39) or medium alone before addition of an agonist (GLP-1, h[Gly^2]GLP-2, or exendin-4). The treated cells were then incubated at 37 °C for 10 min. Absolute ethanol (−20 °C) was added to terminate the reaction, and the plates were stored at −80 °C until the cell extracts were collected (2–4 h later). Forskolin was used as a positive control. cAMP radioimmunoassays (Biomedical Technologies, Inc., Stoughton, MA) were performed on dried aliquots of extract, and data were normalized to cAMP/well. All treatments were performed in triplicate or quadruplicate, and the data are expressed as means ± SD. EC_{50} values were calculated using Prism Version 3.00 (GraphPAD Software Inc., San Diego, CA).

Intracerebroventricular Peptide Injections and Food Intake—For intracerebroventricular injections, adult male CD1 mice randomized into multiple experimental groups were anesthetized by inhalation of methoxyflurane (Metophane, Janssen, Toronto) (43). Following intracerebroventricular injections of equal volumes of saline or peptide dissolved in saline, animals were allowed to recover for ~15 min until the observation of a righting response. Mice were then weighed and given a pre-measured quantity of rodent chow, and food intake was quantified at 1, 2, 4, and 22 h. The accuracy of intracerebroventricular injection was verified at autopsy analysis by detection of bromphenol dye in the lateral ventricles of selected animals. Animals were injected with peptide either at 7 p.m. (for dark-phase feeding studies) or at 10 a.m. following an overnight fast of 15 h (for fasting studies).

RESULTS

The observation that GLP-2R RNA transcripts were restricted to the dorsomedial nucleus of the rat hypothalamus as demonstrated by *in situ* hybridization (35) differed from recent reports of more widespread expression of the GLP-2R in multiple regions of the CNS (37). We detected GLP-2R mRNA transcripts not only in the rat hypothalamus, but also in the brainstem by RT-PCR (34). Accordingly, we reexamined the localization of rodent CNS GLP-2R expression using a combination of RT-PCR and immunohistochemistry analyses. Furthermore, we compared the localization of endogenous GLP-2R mRNA transcripts and GLP-2R immunopositivity with the regions of LacZ expression in tissues isolated from GLP-2R promoter-*lacZ* transgenic mice.

To identify DNA regulatory sequences important for control of CNS GLP-2R expression, we focused initially on characterization of the 5′-end of the GLP-2R mRNA transcript. As GLP-2R cDNA sequences upstream of the translation start site had not been previously reported (33), we carried out 5′-RACE experiments using cDNA template from rat brain to identify 5′-untranslated sequences of the rat GLP-2R. Multiple RACE reaction products were consistently obtained that were ~500 bp in size. These products were cloned, and sequence analysis demonstrated the presence of previously identified rat GLP-2R cDNA sequences (33) and an additional 104 nucleotides of rat GLP-2R 5′-untranslated sequences upstream of the previously reported ATG codon (Fig. 1*a*).

Using a 213-bp *Apa*I/*Sma*I rat cDNA fragment containing 5′-coding sequences as a probe, we isolated an ~2-kb subclone from a bacterial artificial chromosome clone derived from a mouse genomic library. The DNA sequences of the mouse GLP-2R genomic subclone were aligned with the known rat GLP-2R cDNA sequence (33) and with human GLP-2R genomic sequence we identified in the GenBank™/EBI Data Bank, as shown in Fig. 1*b*. The rat and mouse sequences exhibited 96% identity over the first 104 bp 5′ to the initiator ATG codon (rat); the mouse and human GLP-2R cDNAs exhibited 76% identity over this same region. Whereas the rat and human GLP-2R sequences contained an upstream ATG translation initiation site that would give rise to a GLP-2R protein containing an extra 41 amino acids at the N terminus, a more distal ATG initiation codon was identified in the mouse (Fig. 1*b*). Nevertheless, transfection studies using a rat GLP-2R cDNA that initiates translation from the downstream rat ATG codon corresponding to the position of the mouse ATG codon gives rise to a functional GLP-2R (33, 42). Hence, the biological significance of the additional 41 amino acids predicted to be present in the rat and human (but not the mouse) GLP-2R sequences remains unclear.

Using the mouse GLP-2R genomic sequences, we identified genomic sequences in the GenBank™/EBI Data Bank that shared 98% identity over 3103 nucleotides with our murine GLP-2R genomic subclone isolated from BAC DNA. Analysis of the murine GLP-2R genomic sequence in GenBank™/EBI also demonstrated the presence of a single translation initiation codon in the murine gene.

As the glucagon, GLP-1, and GLP-2 receptors are related members of a G protein-coupled receptor superfamily (44), we compared the sequences of the 5′-untranslated and 5′-flanking regions of these three receptors. We did not find significant similarity using base pair matching over 5′-untranslated or putative promoter regions. No putative TATA or CAAT box sequences were identified in the mouse GLP-2R genomic sequences immediately 5′ to the end of the putative 5′-untranslated region. Computer analyses identified several potential transcription factor recognition sites (TFSEARCH Version 1.3) for CdxA, GATA-1, nuclear factor-κB, and Sp1 as indicated in Fig. 1*b*. Comparison of the 5′-flanking regions in the mouse and human GLP-2R genes revealed 70% identity over the first 200 nucleotides 5′ to the start of transcription; however, sequence similarity diverged 5′ to this region.

Although the glucagon and GLP-1 receptor promoters have been characterized in cell transfection experiments *in vitro* (45–48), there is no information available regarding the transcriptional regulation of the genes encoding the glucagon, GLP-1, and GLP-2 receptors *in vivo*. To identify GLP-2R regulatory sequences that direct GLP-2R gene transcription to various regions of the CNS, we ligated an ~1.5-kb fragment of the murine GLP-2R gene containing 5′-flanking and 5′-untranslated sequences upstream of the *lacZ* cDNA (Fig. 1*c*) and generated several lines of GLP-2R promoter-*lacZ* transgenic mice. We then assessed and compared expression of the endogenous murine GLP-2R gene with expression of the *lacZ* transgene in different regions of the murine CNS.

Consistent with the highly tissue-specific expression of the endogenous rat and human GLP-2Rs in the gastrointestinal tract (33, 34), both *lacZ* transgene and endogenous GLP-2R mRNA transcripts were detected in the stomach (data not shown) and in both the small and large bowel (Fig. 2*a*). Similarly, we observed GLP-2R transcripts in several regions of the murine CNS (Fig. 2*b*). Endogenous GLP-2R mRNA and transgene-derived *lacZ* transcripts were identified in the cerebellum, medulla, pons, amygdala, and cerebral cortex of GLP-2R promoter-*lacZ* mice (Fig. 2*b*). In contrast, GLP-2R mRNA transcripts, but not *lacZ* mRNA transcripts, were detected in the pituitary gland.

The results of previous studies localized rat and human GLP-2R transcripts and immunoreactive protein principally to the gastrointestinal tract and CNS (33, 34). Consistent with the tissue specificity of endogenous GLP-2R expression, the

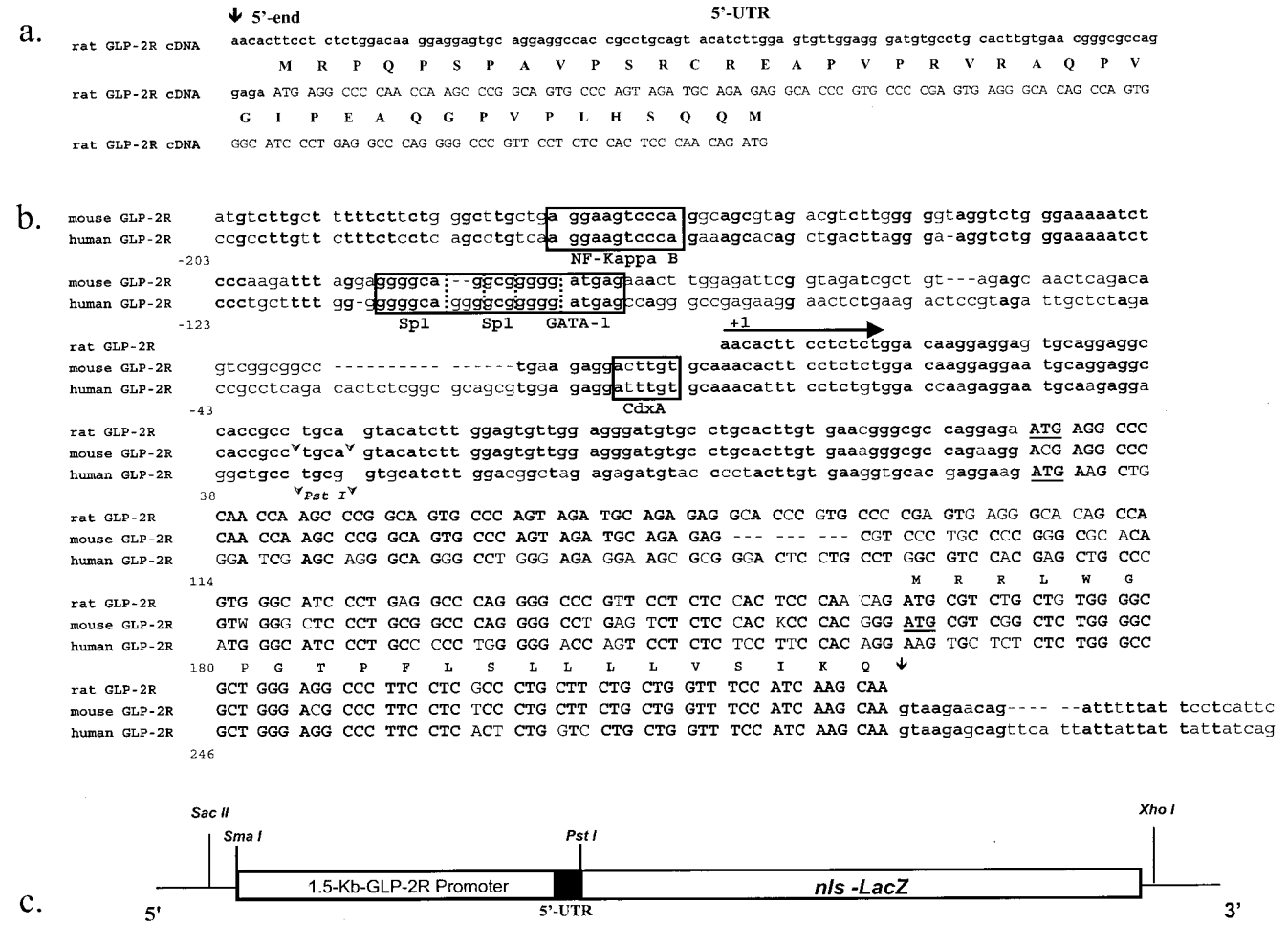

FIG. 1. **Nucleotide sequences at the 5′-end of the GLP-2R mRNA and gene.** *a*, ~230 bp of sequence, including 104 bp of 5′-untranslated sequences corresponding to the 5′-end of the cDNA encoding the rat GLP-2R obtained from sequencing of RACE products, is shown. The *vertical arrow* indicates the 5′-end of the RACE product and the putative start of transcription. The 5′-untranslated region (*5′-UTR*) is highlighted in *boldface letters*. The coding sequence is presented in *uppercase letters*, with the corresponding translated product presented above in *uppercase boldface letters*. *b*, shown is the organization of 5′-flanking and exon 1 sequences in the mouse GLP-2R gene compared with rat exon 1 and human GLP-2R 5′-flanking and 5′-untranslated sequences. Sequence identities are presented in *boldface letters*, and *dashes* indicate gaps introduced to maximize alignment. The DNA sequence is numbered from the putative transcription start site. Potential transcription factor-binding regions in the putative promoter regions of the human and mouse genes are *boxed*. The predicted translation initiation codons in rat, mouse, and human genes are *underlined*. The predicted translated product of the mouse gene is indicated above the nucleotide sequence. The *vertical arrow* indicates the predicted 5′-boundary of intron 1. The *PstI* site, corresponding to the 3′-end of the GLP-2R promoter-*lacZ* transgene, is indicated by *arrowheads*. The *letters K* and *W* are ambiguity codes, where *K* = G or T and *W* = A or T. The GenBank™/EBI accession number for the rat GLP-2R sequences derived from our RACE experiments is AF338223. The accession number for the nucleotide sequence of our mouse GLP-2R genomic clone is AF338224. The accession number for the previously published rat GLP-2R cDNA is AF105368 (33). The accession number for GenBank™/EBI sequences we identified as corresponding to human GLP-2R genomic sequence is AC069006. The accession number for the GenBank™/EBI submission we identified as corresponding to mouse GLP-2R genomic sequence is AC016464. *c*, construction of the transgene was achieved by inserting a 1.5-kb *Sma*I/*Pst*I fragment of the murine GLP-2R gene upstream of nuclear localization signal-containing *lacZ* (*nls-LacZ*) cDNA. The *black box* denotes the presence of GLP-2R 5′-untranslated sequences 5′ to the *Pst*I site shown in *b*. *NF-Kappa B*, nuclear factor-κB.

GLP-2R promoter-*lacZ* transgene was not expressed in the liver, kidney, spleen, or heart of transgenic mice (Fig. 2*c*). The specificity of transgene expression was further illustrated by demonstrating that tissues that did not contain transgene-derived mRNA transcripts also did not contain $LacZ^+$ cell types (Fig. 2*d*). Furthermore, additional evidence for the regional specificity of transgene expression in the CNS derives from analysis of numerous coronal sections of frozen brain tissue from GLP-2R promoter-*lacZ* transgenic mice, the majority of which did not exhibit any β-galactosidase-like immunopositivity when incubated with a β-galactosidase-specific antiserum (Fig. 2*d* and data not shown). Similarly, the majority of coronal sections of frozen brain tissue incubated with anti-GLP-2R antiserum were also immunonegative.

To localize specific regions and cell types within the rat and mouse CNS that express the endogenous GLP-2R, we used immunopurified antiserum directed against the carboxyl-terminal region of the rat GLP-2R. The specificity of this antiserum has been previously characterized (34). The antiserum specifically recognizes the GLP-2R as a single major product of ~72 kDa on Western blot analysis and does not exhibit cross-reactivity against the related glucagon and GLP-1 receptors as demonstrated by the lack of immunopositivity in histological sections of rat liver or pancreas incubated with the anti-GLP-2R antiserum (34). GLP-2R-immunoreactive cells were observed in the Purkinje layer of the rat cerebellum, with no staining detected in other cell types throughout the cerebellum (Fig. 3*a*). GLP-2R-immunoreactive neurons were also detected in the Purkinje cell layer of the murine cerebellum (Fig. 3*c*). In contrast, adjacent sections incubated with preimmune serum (Fig. 3*b*) or without primary antibody did not exhibit immunopositivity in the Purkinje cell layer. Similarly, preabsorption

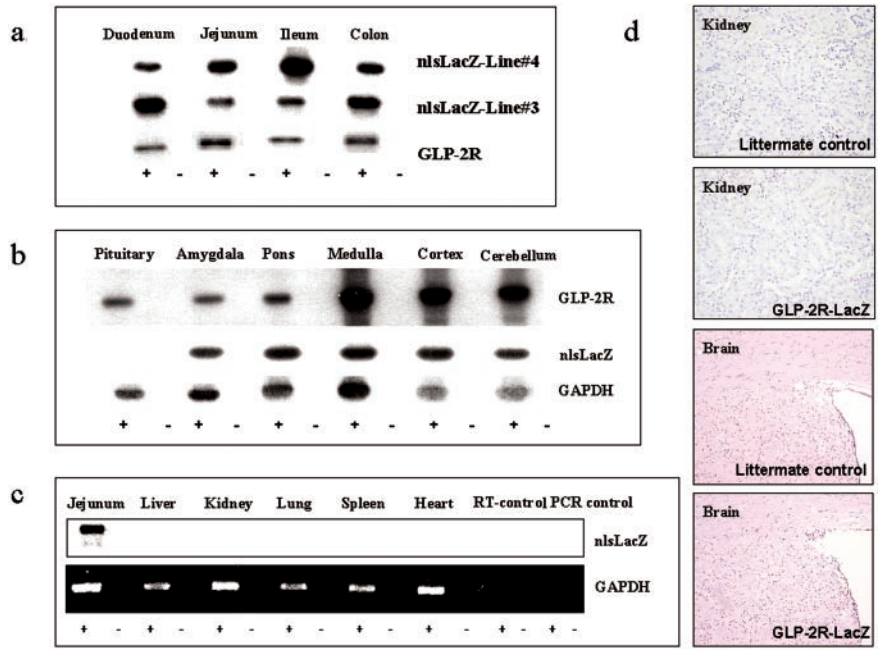

FIG. 2. **RT-PCR analysis of endogenous GLP-2R and GLP-2R promoter-*lacZ* transgene expression in adult mouse tissues.** *a*, RT-PCR analysis of (i) transgene (nuclear localization signal-containing *lacZ* (*nlsLacZ*)) expression in two different lines of 1.5-kb GLP-2R promoter-*lacZ* transgenic mice (lines 3 and 4) and (ii) endogenous GLP-2R mRNA transcripts in gastrointestinal tissues. *b*, RT-PCR analysis of endogenous GLP-2R, GLP-2R promoter-*lacZ* (*nlsLacZ*), and glyceraldehyde-3-phosphate dehydrogenase (*GAPDH*) mRNA transcripts in structures isolated from the CNS of GLP-2R promoter-*lacZ* transgenic mice. *c*, analysis of the tissue specificity of transgene expression in the livers, kidneys, lungs, spleens, and hearts from 1.5-kb GLP-2R promoter-*lacZ* transgenic mice. *PCR control* designates reaction reactions carried out in the absence of cDNA, whereas *RT-control* indicates reactions carried out in the absence of reverse transcriptase. + and −, presence and absence of first-strand cDNA, respectively. *d*, analysis of transgene expression in frozen histological sections (kidney and brain) from 1.5-kb GLP-2R promoter-*lacZ* transgenic mice and littermate control mice incubated with anti-β-galactosidase antiserum.

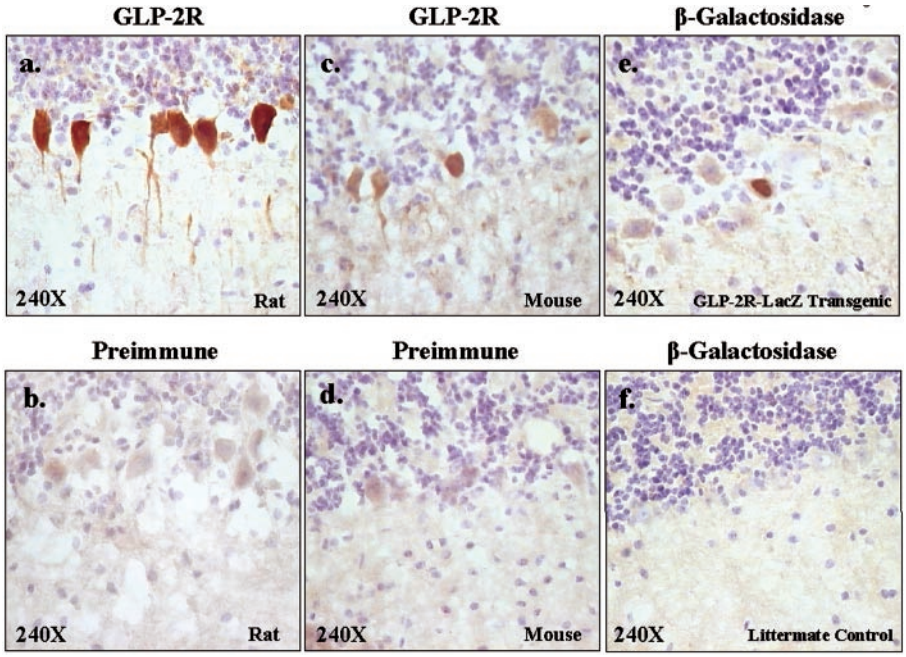

FIG. 3. **Analysis of endogenous GLP-2R and GLP-2R promoter-*lacZ* transgene expression in the cerebellum.** Frozen coronal sections of Formalin-perfused rat (*a* and *b*) and mouse (*c* and *d*) cerebellums were exposed to anti-GLP-2R antiserum or to preimmune serum to detect the specific presence of GLP-2R$^+$ cells. Frozen coronal sections of Formalin-perfused mouse GLP-2R promoter-*lacZ* (*e*) and littermate control (*f*) cerebellums were incubated with a polyclonal antibody generated against the β-galactosidase enzyme to detect specific nuclear LacZ expression in the transgenic cerebellum. Histological regions presented correspond approximately to the coordinates in Fig. 91 in the atlas of Franklin and Paxinos (67).

of anti-GLP-2R antiserum with recombinant GLP-2R protein completely eliminated GLP-2R immunoreactivity in the cerebellum.

Analysis of transgene expression in GLP-2R promoter-*lacZ* transgenic mice demonstrated nuclear LacZ immunopositivity in the Purkinje cell layer of the cerebellum, consistent with the presence of a nuclear localization signal in the modified *lacZ* coding sequence (Fig. 3*e*). In contrast, LacZ$^+$ cells were not detected in the cerebellums of age-matched non-transgenic littermate controls (Fig. 3*f*). Purkinje neurons exhibiting positivity for the native GLP-2R in rat and mouse cerebellums detected with antiserum against the endogenous GLP-2R were comparatively more abundant than the number of LacZ-immunopositive Purkinje neurons identified in the transgenic mouse cerebellum.

As both GLP-2R and GLP-2R promoter-*lacZ* RNA transcripts were detected in extrahypothalamic regions of the rat CNS (Fig. 2*b*), we next examined these regions for GLP-2R immunoreactivity. GLP-2R-immunoreactive cells were detected in the hippocampus and dentate gyrus of the rat CNS (Fig. 4, *a–c*). Numerous GLP-2R-immunoreactive cells were observed in the pyramidal cell layer of the rostral rat hippocampus, including the CA1, CA2, and CA3 fields; in the caudal hippocampus, GLP-2R$^+$ cells were also present in the CA3 fields. GLP-2R-immunoreactive staining was also observed in scattered cell types located in the granular layer and polymorphic hilus region of the rat dentate gyrus. In contrast, preabsorption of antiserum with recombinant GLP-2R or the use of preimmune antiserum did not result in detectable GLP-2R immunopositivity in adjacent serial sections (data not shown).

Following detection of GLP-2R immunopositivity in the rat

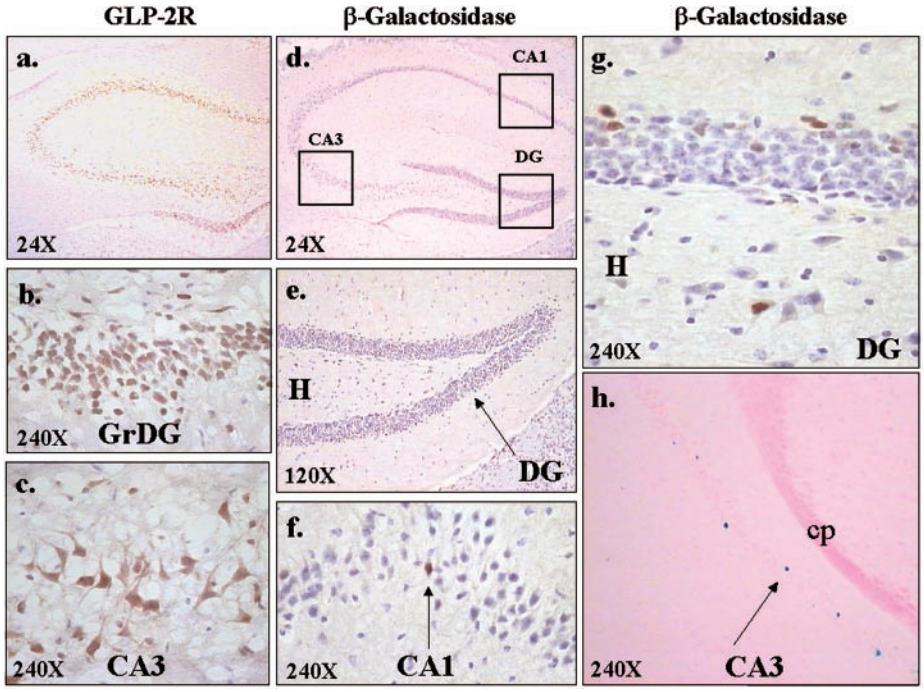

FIG. 4. **Histological analysis of GLP-2R and GLP-2R promoter-*lacZ* transgene expression in the hippocampus and dentate gyrus.** *a–c*, frozen coronal sections of perfused rat brain were incubated with anti-GLP-2R antiserum to detect the presence of GLP-2R$^+$ cell types in the hippocampus and dentate gyrus. Endogenous GLP-2R immunostaining is shown in the rostral hippocampus (*a*), granular layer of the dentate gyrus (*GrDG*; *b*), and CA3 field of the hippocampus (*c*). *d–h*, frozen coronal sections of perfused mouse brain GLP-2R promoter-*lacZ* were incubated with anti-β-galactosidase antibody to identify transgene-positive nuclei in the transgenic hippocampus and dentate gyrus. The *boxed regions* in *d* correspond to areas containing LacZ$^+$ cells, including the transgenic dentate gyrus (*DG*; *e* and *g*) and the CA1 field (*f*) of the transgenic hippocampus using β-galactosidase immunocytochemistry. The caudal CA3 field of the transgenic hippocampus using X-gal histochemical analysis is shown in *h*. The relative magnifications (×24, 120, and 240) are shown in each panel. Histological regions represented in *a–c* correspond approximately to the coordinates in Figs. 40 and 41 in the atlas of Franklin and Paxinos (67); those in *d*, *e*, and *g* correspond approximately to the coordinates in Fig. 43; that in *f* correspond approximately to the coordinates in Fig. 53; and that in *h* correspond approximately to the coordinates in Fig. 59. *H*, hilus region; *cp*, basal cerebral peduncle.

hippocampus and dentate gyrus, we examined these same structures in the CNS of GLP-2R promoter-*lacZ* transgenic mice. Nuclear LacZ immunopositivity was clearly visible within similar cell types (that also exhibited endogenous GLP-2R immunoreactivity) positioned in the hippocampus and dentate gyrus in GLP-2R promoter-*lacZ* transgenic mice (Fig. 4, *d–h*). Corresponding age-matched littermate non-transgenic control sections did not exhibit LacZ immunopositivity under identical staining conditions. In contrast to the extent of endogenous GLP-2R immunoreactivity observed in the pyramidal layers of the rat hippocampus, LacZ-immunopositive cells in the CA1, CA2, and CA3 fields of the transgenic hippocampus were less abundant, with the highest density of positive cells observed in the CA3 field (Fig. 4*h*). Nevertheless, β-galactosidase-positive cells were dense in the granular layer of the transgenic dentate gyrus (Fig. 4*g*). Cells with nuclear β-galactosidase staining were also observed in the polymorphic hilus region of the transgenic dentate gyrus, consistent with the distribution of GLP-2R$^+$ cells observed in the rat dentate gyrus using anti-GLP-2R antiserum.

Examination of the CNS in GLP-2R promoter-*lacZ* transgenic mice revealed additional structures that exhibited intense β-galactosidase activity. The amygdala contained a number of LacZ$^+$ cells detected bihemispherically by both histochemical and immunocytochemical staining (Fig. 5, *a–c*). Positive cell staining was principally restricted to the posterolateral and posteromedial cortical amygdaloid nuclei and to the amygdalohippocampal area. The lateral and medial amygdaloid nuclei did not contain positive staining.

The results of previous GLP-2R *in situ* hybridization studies demonstrated restricted hypothalamic GLP-2R expression exclusively in the caudal part of the rat dorsomedial nucleus of the hypothalamus (35). Immunocytochemical analysis of the transgenic hypothalamus revealed occasional rare LacZ$^+$ nuclei of the dorsomedial nucleus (Fig. 5*d*). A few rare LacZ$^+$ nuclei were also detected throughout the ventromedial hypothalamic nucleus in transgenic mice (Fig. 5, *e* and *f*).

Neural populations exhibiting nuclear β-galactosidase activity were also localized to the thalamic nuclei of GLP-2R promoter-*lacZ* transgenic mice (Fig. 5, *g* and *h*). Nuclear LacZ immunopositivity was observed in select cells in the mediodorsal thalamic nucleus and in the ventrolateral and dorsomedial parts of the laterodorsal thalamic nucleus. Immunopositivity was also observed in the ventrolateral geniculate nucleus, with the majority of positive cells in the parvocellular regions (Fig. 5*i*). A few immunopositive cells were identified in the caudate putamen, dorsal fornix, and septofimbrial nucleus of GLP-2R promoter-*lacZ* mice. Nuclear β-galactosidase positivity was also detected in cells at the base of the corpus callosum in the ventral endopiriform nucleus and in the piriform cortex (data not shown). A summary of the sites of endogenous GLP-2R and GLP-2R promoter-*lacZ* transgene expression is shown in Table I.

As intracerebroventricular GLP-2 administration inhibits dark-phase feeding in rats (35), we compared the effects of a dipeptidyl peptidase IV-resistant GLP-2 analog, h[Gly^2]GLP-2 (40), with the GLP-1 analog exendin-4 on feeding after a prolonged fast or during dark-phase feeding in mice. The GLP-1 analog exendin-4, but not h[Gly^2]GLP-2, inhibited food intake in fasted mice (Fig. 6*a*). In contrast, both exendin-4 and h[Gly^2]GLP-2 significantly inhibited dark-phase food intake (Fig. 6*b*), although the inhibitory effects of exendin-4 were significantly more potent than those of the GLP-2 analog. Similarly, whereas the inhibitory effects of exendin-4 were sustained over 24 h, the inhibitory effects of h[Gly^2]GLP-2 on food

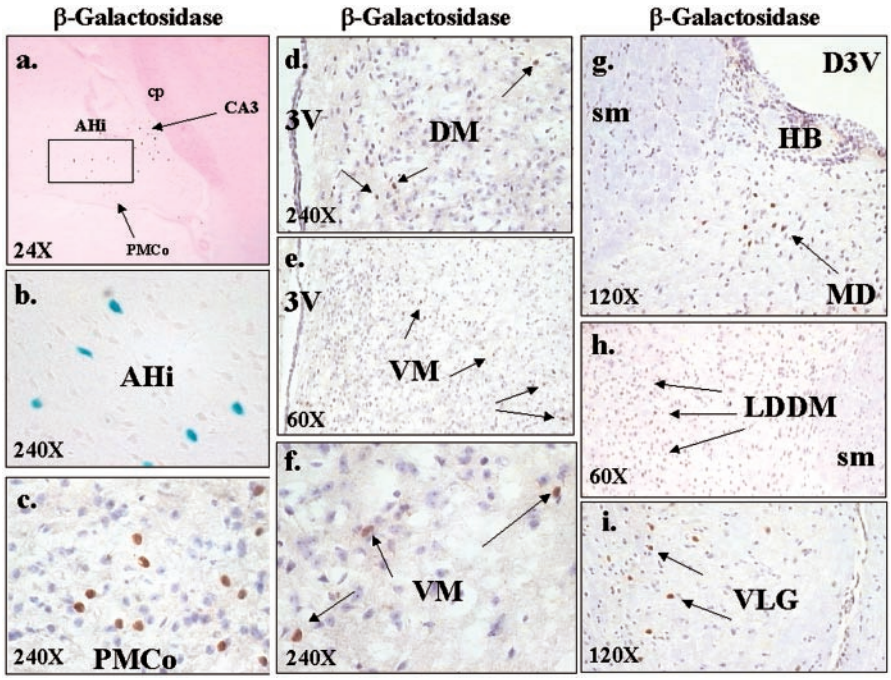

FIG. 5. **Histological analysis of GLP-2R promoter-*lacZ* expression in the amygdaloid, hypothalamic, and thalamic nuclei of transgenic mice.** *a*, histochemical analysis of LacZ positivity in the amygdaloid nucleus of GLP-2R promoter-*lacZ* transgenic mice using X-gal staining. The *boxed area* corresponds to $LacZ^+$ nuclei in the amygdalohippocampal area, and the *arrows* point to $LacZ^+$ nuclei in the caudal CA3 region of the hippocampus and the posteromedial cortical amygdaloid nucleus. *b* and *c*, immunocytochemical analysis of the amygdalohippocampal area (*b*) and the posteromedial cortical amygdaloid nucleus (*c*) using an antibody directed against the β-galactosidase enzyme. *d–f*, immunocytochemical analysis of the hypothalamus of GLP-2R promoter-*lacZ* transgenic mice using anti-β-galactosidase antiserum, specifically in the dorsomedial nucleus (*d*) and in the ventromedial nucleus (magnification × 60 (*e*) and 240 (*f*)). *g–i*, immunocytochemical analysis of thalamic nuclei in GLP-2R promoter-*lacZ* transgenic mice using anti-β-galactosidase antiserum, specifically in the mediodorsal nuclei, the dorsomedial part of the laterodorsal thalamic nucleus, and the ventrolateral geniculate nucleus, respectively. The *arrows* point to $LacZ^+$ nuclei. The relative magnifications (×24, 60, 120, and 240) are indicated. Histological regions presented in *a–c* correspond approximately to the coordinates in Figs. 51 and 52 in the atlas of Franklin and Paxinos (67); those in *d–f* correspond approximately to the coordinates in Figs. 46 and 47; that in *g* corresponds approximately to the coordinates in Fig. 38; that in *h* corresponds approximately to the coordinates in Fig. 41; and that in *i* corresponds approximately to the coordinates in Figs. 46 and 47. *AHi*, amygdalohippocampal area; *PMCo*, posteromedial cortical amygdaloid nucleus; *cp*, basal cerebral peduncle; *DM*, dorsomedial hypothalamic nucleus; *VM*, ventromedial hypothalamic nucleus; *3V*, third ventricle; *D3V*, dorsal third ventricle; *HB*, habenular nucleus; *sm*, stria medullaris; *MD*, mediodorsal thalamic nucleus; *LDDM*, dorsomedial part of the laterodorsal thalamic nucleus; *VLG*, ventrolateral geniculate nucleus.

TABLE I

Analysis of endogenous GLP-2R and GLP-2R promoter-lacZ transgene expression in rodent brain, bowel, and peripheral tissues

Endogenous GLP-2R and GLP-2R promoter-*lacZ* transgene expression was examined in rodent brain, gastrointestinal tract, and peripheral tissues using a combination of RT-PCR and immunocytochemistry analyses. Analysis of 1.5-kb GLP-2R promoter-*lacZ* transgene expression in brain tissues was performed in three independent transgenic lines using X-gal histochemical analysis. Transgene expression in gastrointestinal tissues was also performed in all three independent transgenic lines using RT-PCR analysis. Transgene expression was observed in the amygdala, hippocampus, and dentate gyrus by histochemistry in all three lines. Immunocytochemistry for β-galactosidase was used to analyze in more detail the cellular localization of CNS transgene expression in one line of GLP-2R promoter-*lacZ* transgenic mice. PT, pituitary; AM, amygdala; HC, hippocampus; DG, dentate gyrus; HY, hypothalamus; P, pons; MD, medulla; CX, cortex; CB, cerebellum; ST, stomach; DU, duodenum; JE, jejunum; IL, ileum; CL, colon; LV, liver; KD, kidney; LG, lung; SP, spleen; HT, heart. +, expression; −, lack of expression.

	Brain									Bowel					Peripheral tissues				
	PT	AM	HC	DG	HY	P	MD	CX	CB	ST	DU	JE	IL	CL	LV	KD	LG	SP	HT
Endogenous GLP-2R	+	+	+	+	+	+	+	+	+	+	+	+	+	+	−	−	+	−	−
lacZ transgene	−	+	+	+	+	+	+	+	+	+	+	+	+	+	−	−	−	−	−

intake were transient and not detectable after >4 h (data not shown).

The effects of GLP-2 on food intake in rats were completely blocked by the GLP-1R antagonist exendin-(9–39), suggesting that exendin-(9–39) might function as a GLP-2 antagonist *in vivo* (35). Remarkably, the inhibitory effects of intracerebroventricular h[Gly^2]GLP-2 on food intake in wild-type mice were significantly more pronounced in the presence of co-administered exendin-(9–39) at multiple time intervals (Fig. 6*c*), including the first hour. In contrast, in the absence of exendin-(9–39), intracerebroventricular h[Gly^2]GLP-2 did not inhibit food intake in the first hour after peptide injection (Fig. 6, *b* and *c*). Furthermore, as little as 0.05 μg of exendin-(9–39) was sufficient for significant potentiation of the anorectic effects of h[Gly^2]GLP-2 on the inhibition of dark-phase food intake at the 1–2-h time point (Fig. 6*d*).

The demonstration that the GLP-1R antagonist exendin-(9–39) significantly enhanced the anorectic effect of GLP-2 in wild-type mice implied a role for GLP-1R signaling in the regulation of CNS GLP-2 action. Accordingly, we next examined the effects of intracerebroventricular h[Gly^2]GLP-2 in mice with complete genetic disruption of GLP-1R signaling (43). Remarkably, $GLP\text{-}1R^{-/-}$ mice exhibited a significantly greater sensitivity to the inhibitory actions of the GLP-2 analog on food intake, as can clearly be seen at the 0–1- and 2–4-h time points, compared with the anorectic effects of an identical amount of intracerebroventricular h[Gly^2]GLP-2 administered to wild-type control mice (Fig. 6*e*).

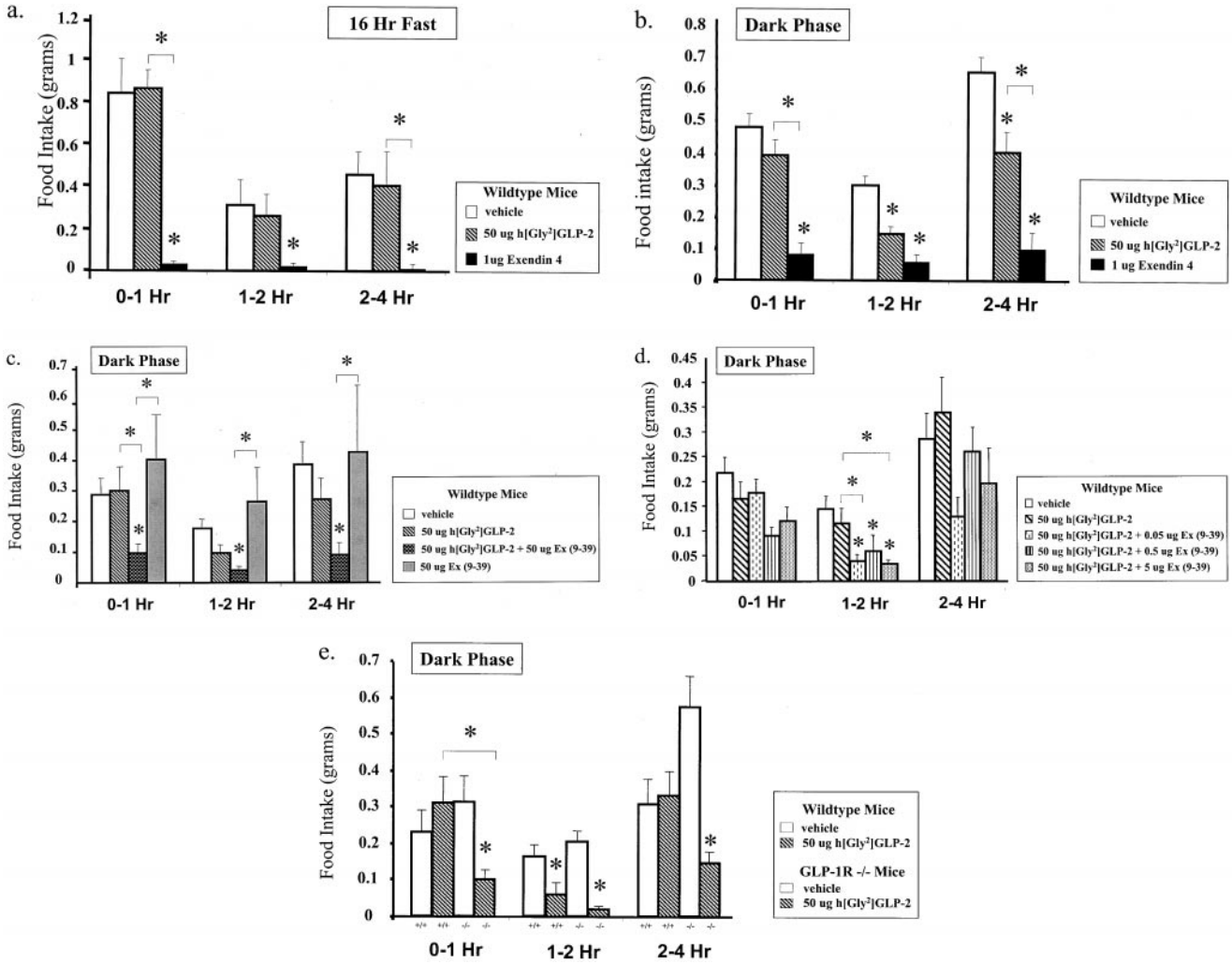

FIG. 6. **h[Gly^2]GLP-2 inhibits dark-phase food intake in mice.** *a* and *b*, mice were randomized into three groups and received an intracerebroventricular injection of vehicle (PBS), h[Gly^2]GLP-2 (50 μg dissolved in PBS), or exendin-4 (1 μg dissolved in PBS) following a 15-h fast (*a*) or prior to the start of the dark phase (*b*). Following recovery, food intake was measured at 1, 2, and 4 h after injection. Values are expressed as means ± S.E. (n = 6 for *a* and n = 8–20 for *b*). *c*, groups of wild-type mice were administered vehicle (PBS), h[Gly^2]GLP-2 (50 μg dissolved in PBS), h[Gly^2]GLP-2 and exendin-(9–39) (*Ex (9–39)*) (50 μg of each peptide dissolved in PBS), or exendin-(9–39) alone (50 μg dissolved in PBS) via intracerebroventricular injection. *d*, groups of wild-type mice were administered intracerebroventricularly vehicle (PBS), h[Gly^2]GLP-2 alone (50 μg dissolved in PBS), or h[Gly^2]GLP-2 (50 μg dissolved in PBS) and exendin-(9–39) (0.05, 0.5, or 5 μg dissolved in PBS). *e*, groups of wild-type and GLP-1R$^{-/-}$ mice were injected intracerebroventricularly with either vehicle (PBS) or h[Gly^2]GLP-2 (50 μg dissolved in PBS) just prior to the start of the dark phase, and food intake was measured at 1, 2, and 4 h. Data are expressed as means ± S.E. (n = 5–8). Treatments at each time point for all panels were compared using a one-way analysis of variance, followed by a least significant difference multiple range test using SPSS for Windows Version 5.0.1 (SPSS Inc., Chicago, IL). *, $p < 0.05$ compared with controls (PBS) or with comparisons between groups indicated by *brackets*.

As the GLP-2-mediated inhibition of food intake is blocked by the GLP-1R antagonist exendin-(9–39) in rats (35), we examined whether exendin-(9–39) functions as a rat GLP-2R antagonist using cells expressing the cloned rat GLP-2R *in vitro*. Although h[Gly^2]GLP-2 increased cAMP accumulation in a dose-dependent manner in BHK-GLP-2R cells, increasing amounts of exendin-(9–39) from 50 to 1000 nM had no effect on h[Gly^2]GLP-2-stimulated cAMP formation (Fig. 7). Exendin-(9–39) alone did not stimulate cAMP accumulation in BHK-GLP-2R cells (data not shown). Furthermore, the GLP-2R responded specifically to h[Gly^2]GLP-2, as no cAMP accumulation was detected following incubation of BHK-GLP-2R cells with GLP-1 or exendin-4 (Fig. 7*a*). In contrast, exendin-(9–39) decreased GLP-1-stimulated cAMP accumulation in a concentration-dependent manner in BHK-GLP-1R cells (Fig. 7*b*), consistent with its known actions as a GLP-1R antagonist. Furthermore, the actions of h[Gly^2]GLP-2 were specific for cells expressing the GLP-2R, as h[Gly^2]GLP-2 had no effect on cAMP accumulation in BHK-GLP-1R cells (Fig. 7).

DISCUSSION

Several lines of evidence support a role for glucagon-like peptides in the control of food intake. Intracerebroventricular administration of GLP-1 agonists inhibits food intake in mice and rats (24, 36, 43), whereas peripheral administration of GLP-1 reduces appetite and size of meal ingestion in human subjects (30, 49). Furthermore, intracerebroventricular administration of the GLP-1R antagonist exendin-(9–39) increases food intake in short-term studies (24) and promotes weight gain in rats after 6 days of intracerebroventricular administration *in vivo* (50). Nevertheless, GLP-1R$^{-/-}$ mice are not obese, do not eat more than wild-type mice, and fail to develop obesity even following several months of high-fat feeding (43, 51). Hence, it remains unclear whether the anorectic effects of intracerebroventricular GLP-1 represent a highly specific effect on CNS feeding centers or a nonspecific effect on CNS nuclei that mediate the response to aversive stimulation (29, 52–55). The available evidence suggests that although intra-

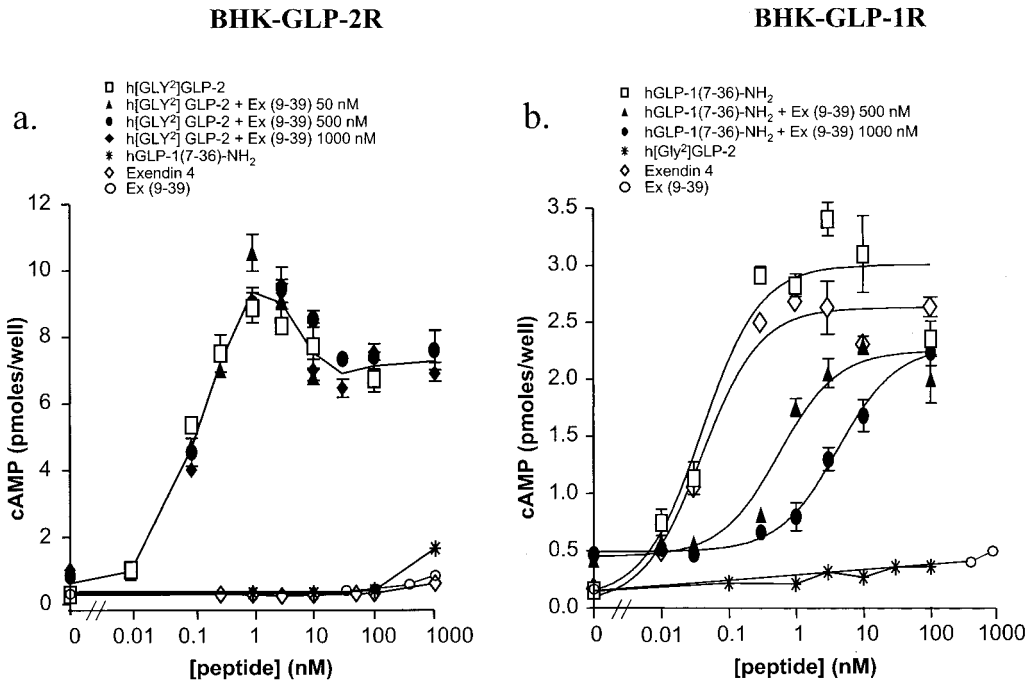

FIG. 7. **Exendin-(9–39) is a specific GLP-1R antagonist in BHK fibroblasts expressing the cloned GLP-1R.** Stably transfected BHK cells expressing either the rat GLP-2R (*a*) or GLP-1R (*b*) were pretreated for 5 min with exendin-(9–39) (*Ex (9–39)*) or medium alone before a 10-min incubation with a receptor agonist: human GLP-1 (*hGLP-1*)-(7–36)-NH_2, exendin-4, or h[Gly^2]GLP-2. Peptides were diluted in Dulbecco's modified Eagle's medium containing 100 μM 3-isobutyl-1-methylxanthine. The cAMP concentration in aliquots of the ethanol extract was determined using a radioimmunoassay and normalized to show cAMP/well. EC_{50} values for h[Gly^2]GLP-2 in the presence of 0, 50, 500, or 1000 nM exendin-(9–39) were 0.044, 0.059, 0.076, and 0.081 nM, respectively. A one-way analysis of variance showed no significant difference among pretreatment conditions of the GLP-2R with exendin-(9–39) at all h[Gly^2]GLP-2 concentrations. A two-factor analysis of variance of the exendin-(9–39) antagonism of the GLP-1R showed a significant difference among pretreatment conditions, human GLP-1-(7–36)-NH_2 concentration, and the interaction between them ($p < 0.001$ for all groups). The EC_{50} value for human GLP-1-(7–36)-NH_2 alone was 0.041 nM, whereas in the presence of 500 or 1000 nM exendin-(9–39), the EC_{50} values were 0.57 and 4.28 nM, respectively. The EC_{50} for exendin-4 in BHK-GLP-1R cells was 0.041 nM. Representative data from two separate experiments performed in triplicate are shown. The concentration of peptide is plotted on a logarithmic scale. *Error bars* represent means ± S.D.

cerebroventricular GLP-1 transiently inhibits food intake (52), GLP-1 does not appear to be an essential regulator of long-term body weight homeostasis *in vivo*.

The report that intracerebroventricular injection of GLP-2 inhibits food intake in rats (35) provides new information about a possible role for GLP-2 in the CNS. Although our data demonstrate that GLP-2 transiently inhibits dark-phase feeding in mice, in contrast to the inhibition of food intake observed with exendin-4, we did not detect significant effects of GLP-2 on inhibition of food intake in mice after a 15-h fast. Furthermore, our data clearly show that the effect of GLP-2 on dark-phase food intake is not blocked, but is significantly enhanced in wild-type mice in the presence of exendin-(9–39), a GLP-1R antagonist (56).

Consistent with the results obtained in wild-type mice following GLP-1R blockade with exendin-(9–39), GLP-2 more potently inhibited food intake in GLP-$1R^{-/-}$ mice compared with wild-type control mice. Hence, our data clearly demonstrate that in contrast to results obtained in rats (35), the effects of GLP-2 on food intake in mice are not attenuated by disruption of GLP-1R signaling. Moreover, transient blockade of the GLP-1R with exendin-(9–39) or complete disruption of GLP-1R signaling in GLP-$1R^{-/-}$ mice was associated with enhanced sensitivity to the inhibitory response to GLP-2. These findings provide new evidence for potential functional cross-talk between GLP-1R and GLP-2R signaling networks regulating food intake *in vivo*, as illustrated in Fig. 8. Whether GLP-1R signaling modulates GLP-2R action directly through intercellular connections or more indirectly through intervening interneuronal connections or by other mechanisms and pathways yet to be described remains to be determined. Nevertheless, our data

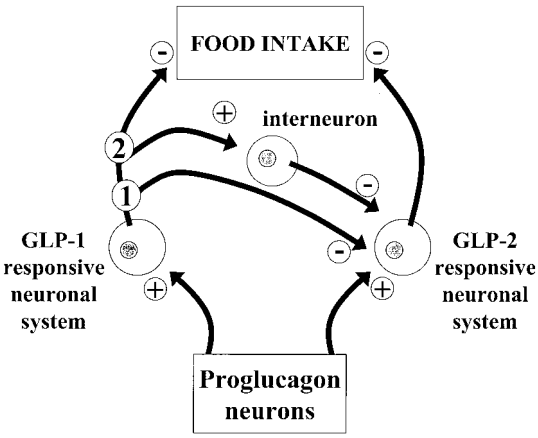

FIG. 8. **Model illustrating the possible interaction between GLP-1- and GLP-2-responsive neuronal systems in the regulation of food intake in the murine CNS.** Both GLP-1 and GLP-2 act to inhibit food intake. The GLP-1-responsive pathway has an inhibitory influence upon the GLP-2-responsive neuronal system either directly as proposed in *Step 1* or through intervening neural systems as shown in *Step 2*. Interruption or attenuation of the GLP-1-responsive pathway leads to a potentiation of the inhibitory action of GLP-2 on food intake. +, excitatory influence; −, inhibitory influence.

strongly implicate the GLP-1R in tonic repression of GLP-2R signaling in the murine CNS.

The finding that the GLP-1R antagonist exendin-(9–39) eliminates the GLP-2-mediated feeding response in rats (35) implies that exendin-(9–39) might also be a functional antagonist of GLP-2 action in the CNS. These observations suggest either that exendin-(9–39) blocks the CNS action of GLP-2 at

the level of the GLP-2R or, alternatively, that GLP-2 may mediate its effects indirectly, through downstream activation of the GLP-1R. Our data in wild-type mice co-injected with h[Gly^2]GLP-2 and exendin-(9–39), taken together with studies using cloned GLP-2 and GLP-1 receptors, clearly demonstrate that exendin-(9–39) is not a functional antagonist of the GLP-2R *in vivo* or *in vitro*. Furthermore, the demonstration that h[Gly^2]GLP-2 inhibits food intake in GLP-1R$^{-/-}$ mice, taken together with the enhanced sensitivity to GLP-2 action following inhibition of GLP-1 signaling, provides new evidence demonstrating that the effects of GLP-2 on feeding do not require the GLP-1R, but may be modulated in part through the functional activity of GLP-1R signaling.

In the rat CNS, proglucagon mRNA transcripts have been localized primarily in the caudal part of the nucleus of the solitary tract, dorsal and ventral medullae, and olfactory bulb (20, 22) and, to a lesser extent, in the hypothalamus (19). In contrast, GLP-1R mRNA transcripts and GLP-1-binding sites are more widely distributed throughout the CNS in the olfactory bulb, temporal cortex, hypothalamus, amygdala, hippocampus, preoptic area, thalamus, substantia nigra, parabrachial nuclei, locus ceruleus, nucleus of the solitary tract, and the area postrema (21, 22, 57). Moreover, GLP-1-immunoreactive tracts originating from the brainstem project to several forebrain nuclei, including the dorsomedial and paraventricular nuclei of the hypothalamus and thalamic and cortical areas (21). Hence, the available evidence demonstrates both GLP-1R expression and GLP-1-immunoreactive tracts in multiple regions of the CNS, including the hypothalamus, amygdala, hippocampus, thalamus, and multiple hindbrain regions. As GLP-1 and GLP-2 are co-synthesized from a common proglucagon precursor, it seems likely that many of the GLP-1-immunopositive tracts originating from the brainstem also contain GLP-2.

The GLP-2R was originally cloned from intestinal and hypothalamic cDNA libraries (33). GLP-2R mRNA transcripts were detected in the rat hypothalamus and brainstem by RT-PCR analysis (34), and GLP-2R expression was exclusively localized to the compact part of the dorsomedial nucleus of the hypothalamus by *in situ* hybridization (35). We have now extended these studies in the rat CNS to demonstrate more widespread distribution GLP-2R expression in thalamic, hippocampal, cortical, and hindbrain regions, in addition to the hypothalamic sites of GLP-2R expression. Our studies our consistent with previous reports demonstrating both GLP-1R and GLP-2R expression in the hypothalamus, midbrain, hippocampus, striatum, and cortex (37), raising the possibility that in the rat CNS, the GLP-1R and GLP-2R are likely expressed in either identical or proximal neural cells in these same brain regions. Furthermore, the demonstrated specificity of the anti-GLP-2R antiserum (34), taken together with the colocalization of endogenous GLP-2R immunoreactivity and nuclear localization of transgenic LacZ expression in multiple CNS regions of the mouse, provides additional evidence supporting a more widespread GLP-2R expression pattern extending beyond the hypothalamus.

The mechanisms regulating expression of the receptors for glucagon, GLP-1, and GLP-2 have not been extensively examined. Although promoter sequences directing expression of the glucagon and GLP-1 receptor sequences have been analyzed in cell-based transfection studies (45, 48), the DNA regulatory sequences mediating tissue-specific control of these receptor genes *in vivo* have not yet been identified. Furthermore, our analysis of the 5′-ends of the receptor coding regions and the 5′-untranslated and 5′-flanking region DNA sequences did not reveal significant shared nucleotide identity across the glucagon, GLP-1, and GLP-2 receptors, providing indirect evidence for the evolution of distinct control mechanisms regulating the transcription of each receptor gene. This observation is supported by a recent examination of the evolution of the receptor DNA sequences for the proglucagon-derived peptides (58), which suggested that these receptors likely evolved independently of each other.

Our results extend the previously reported GLP-2R sequence at the 5′-end and identify both the 5′-untranslated region and the location of intron 1. Furthermore, we provide functional evidence for the transcriptional activity of DNA regulatory sequences in the mouse GLP-2R 5′-flanking region. Our findings demonstrate that an ~1.5-kb fragment of the mouse GLP-2R gene containing 5′-flanking and 5′-untranslated sequences directs transgene expression specifically to the gastrointestinal tract and brain, in agreement with the restricted pattern of tissue-specific expression demonstrated for the endogenous GLP-2R (33, 34). The identification of potential Sp1-binding sites in the proximal GLP-2R promoter is intriguing in light of studies suggesting the functional importance of Sp1-binding sites for basal GLP-1R transcription in transfection studies *in vitro* (47). Furthermore, several studies have demonstrated an important role for both GATA factors and caudal proteins (Fig. 1*b*) in the regulation of both intestine- and enteroendocrine-specific gene transcription (59–62). Hence, future studies examining the potential functional importance of these sites for regulation of GLP-2R gene transcription appear warranted.

The regional and tissue-specific localization of GLP-2R promoter-*lacZ* expression was highly correlated with the expression of the endogenous murine GLP-2R, with the exception of the pituitary gland and lung. The abundance of cells expressing the endogenous GLP-2R appeared comparatively greater than the number of cells expressing the GLP-2R promoter-*lacZ* transgene in regions such as the hippocampus and cerebellum. These findings imply that additional DNA regulatory sequences not present in the 1.5-kb GLP-2R 5′-flanking region are required to correctly specify transgene expression in all cells and tissues expressing the endogenous GLP-2R. Furthermore, the interpretation of the localization data may be further complicated in that unlike the endogenous GLP-2R, the nuclear LacZ reporter protein would not be transported to sites distal from the neural nuclei that transcribe the GLP-2R promoter *in vivo*. Nevertheless, the excellent correlation between gastrointestinal tissues and CNS regions expressing both the endogenous GLP-2R and the *lacZ* transgene suggests that putative regulatory sequences encoded within the first 1.5 kb of the mouse GLP-2R promoter may be useful for future studies directing transgenes to specific GLP-2R$^+$ cell populations in the murine CNS and gut.

In the gastrointestinal tract, GLP-1 and GLP-2 exert both overlapping and distinct actions in the regulation of nutrient absorption and glucose homeostasis (2). Although both GLP-1 and GLP-2 inhibit gastric emptying and gastric acid secretion, the mechanisms underlying the common actions of these peptides have not been delineated. Despite these overlapping actions, however, no previous studies have implicated a role for GLP-1R signaling in the regulation of GLP-2 action *in vivo*. Our data generated independently using either the GLP-1R antagonist exendin-(9–39) or GLP-1R$^{-/-}$ mice clearly show that blockade or disruption of GLP-1 signaling enhances the sensitivity to GLP-2 action in the murine CNS. Given the overlapping actions and expression patterns of GLP-1 and GLP-2 in peripheral tissues and brain, it seems reasonable to search for additional interactions of GLP-1R and GLP-2R signaling systems in the control of shared physiological actions

such as gastric emptying or gastric acid secretion (11, 12).

Following the initial description of GLP-1 action in the rodent CNS as a satiety factor, multiple additional actions for GLP-1 in the CNS have emerged, including regulation of hypothalamic pituitary function (25, 26, 63, 64), modulation of the extent of brain injury (65), and transduction of the CNS response to aversive stimulation (28, 66). Our data demonstrating expression of the GLP-2R in multiple regions of the rodent CNS are consistent with previous findings demonstrating extensive projections of GLP-1- and GLP-2-immunopositive nerve fibers to comparable regions of the rat brain (21). Taken together, the available data clearly imply additional potential roles for CNS GLP-2, beyond hypothalamic regulation of food intake, that merit careful analysis in future studies.

Acknowledgment—We thank Dr. D. Irwin for help with DNA sequence analysis and review of the manuscript.

REFERENCES

1. Mojsov, S., Heinrich, G., Wilson, I. B., Ravazzola, M., Orci, L., and Habener, J. F. (1986) *J. Biol. Chem.* **261,** 11880–11889
2. Drucker, D. J. (1998) *Diabetes* **47,** 159–169
3. Drucker, D. J. (2001) *Endocrinology* **142,** 521–527
4. Holst, J. J. (1999) *Trends Endocrinol. Metab.* **10,** 229–235
5. Kieffer, T. J., and Habener, J. F. (1999) *Endocr. Rev.* **20,** 876–913
6. Xu, G., Stoffers, D. A., Habener, J. F., and Bonner-Weir, S. (1999) *Diabetes* **48,** 2270–2276
7. Stoffers, D. A., Kieffer, T. J., Hussain, M. A., Drucker, D. J., Egan, J. M., Bonner-Weir, S., and Habener, J. F. (2000) *Diabetes* **49,** 741–748
8. Drucker, D. J., Ehrlich, P., Asa, S. L., and Brubaker, P. L. (1996) *Proc. Natl. Acad. Sci. U. S. A.* **93,** 7911–7916
9. Tsai, C.-H., Hill, M., and Drucker, D. J. (1997) *Am. J. Physiol.* **272,** G662–G668
10. Tsai, C.-H., Hill, M., Asa, S. L., Brubaker, P. L., and Drucker, D. J. (1997) *Am. J. Physiol.* **273,** E77–E84
11. Wojdemann, M., Wettergren, A., Hartmann, B., and Holst, J. J. (1998) *Scand. J. Gastroenterol.* **33,** 828–832
12. Wojdemann, M., Wettergren, A., Hartmann, B., Hilsted, L., and Holst, J. J. (1999) *J. Clin. Endocrinol. Metab.* **84,** 2513–2517
13. Benjamin, M. A., McKay, D. M., Yang, P. C., Cameron, H., and Perdue, M. H. (2000) *Gut* **47,** 112–119
14. Cheeseman, C. I., and Tsang, R. (1996) *Am. J. Physiol.* **271,** G477–G482
15. Drucker, D. J., Yusta, B., Boushey, R. P., Deforest, L., and Brubaker, P. L. (1999) *Am. J. Physiol.* **276,** G79–G91
16. Boushey, R. P., Yusta, B., and Drucker, D. J. (1999) *Am. J. Physiol.* **277,** E937–E947
17. Alavi, K., Schwartz, M. Z., Palazzo, J. P., and Prasad, R. (2000) *J. Pediatr. Surg.* **35,** 847–851
18. Prasad, R., Alavi, K., and Schwartz, M. Z. (2000) *J. Pediatr. Surg.* **35,** 357–359
19. Drucker, D. J., and Asa, S. (1988) *J. Biol. Chem.* **263,** 13475–13478
20. Han, V. K. M., Hynes, M. A., Jin, C., Towle, A. C., Lauder, J. M., and Lund, P. K. (1986) *J. Neurosci. Res.* **16,** 97–107
21. Larsen, P. J., Tang-Christensen, M., Holst, J. J., and Orskov, C. (1997) *Neuroscience* **77,** 257–270
22. Merchenthaler, I., Lane, M., and Shughrue, P. (1999) *J. Comp. Neurol.* **403,** 261–280
23. Campos, R. V., Lee, Y. C., and Drucker, D. J. (1994) *Endocrinology* **134,** 2156–2164
24. Turton, M. D., O'Shea, D., Gunn, I., Beak, S. A., Edwards, C. M. B., Meeran, K., Choi, S. J., Taylor, G. M., Heath, M. M., Lambert, P. D., Wilding, J. P. H., Smith, D. M., Ghatei, M. A., Herbert, J., and Bloom, S. R. (1996) *Nature* **379,** 69–72
25. Beak, S. A., Heath, M. M., Small, C. J., Morgan, D. G. A., Ghatei, M. A., Taylor, A. D., Buckingham, J. C., Bloom, S. R., and Smith, D. M. (1998) *J. Clin. Invest.* **101,** 1334–1341
26. Beak, S. A., Small, C. J., Ilovaiskaia, I., Hurley, J. D., Ghatei, M. A., Bloom, S. R., and Smith, D. M. (1996) *Endocrinology* **137,** 4130–4138
27. Seeley, R. J., Blake, K., Rushing, P. A., Benoit, S., Eng, J., Woods, S. C., and D'Alessio, D. (2000) *J. Neurosci.* **20,** 1616–1621
28. Seeley, R. J., Woods, S. C., and D'Alessio, D. (2000) *Endocrinology* **141,** 473–475
29. Rinaman, L. (1999) *Am. J. Physiol.* **277,** R582–R590
30. Toft-Nielsen, M. B., Madsbad, S., and Holst, J. J. (1999) *Diabetes Care* **22,** 1137–1143
31. Szayna, M., Doyle, M. E., Betkey, J. A., Holloway, H. W., Spencer, R. G., Greig, N. H., and Egan, J. M. (2000) *Endocrinology* **141,** 1936–1941
32. Hoosein, N. M., and Gurd, R. S. (1984) *FEBS Lett.* **178,** 83–86
33. Munroe, D. G., Gupta, A. K., Kooshesh, P., Rizkalla, G., Wang, H., Demchyshyn, L., Yang, Z.-J., Kamboj, R. K., Chen, H., McCallum, K., Sumner-Smith, M., Drucker, D. J., and Crivici, A. (1999) *Proc. Natl. Acad. Sci. U. S. A.* **96,** 1569–1573
34. Yusta, B., Huang, L., Munroe, D., Wolff, G., Fantaske, R., Sharma, S., Demchyshyn, L., Asa, S. L., and Drucker, D. J. (2000) *Gastroenterology* **119,** 744–755
35. Tang-Christensen, M., Larsen, P. J., Thulesen, J., Romer, J., and Vrang, N. (2000) *Nat. Med.* **6,** 802–807
36. Tang-Christensen, M., Larsen, P. J., Goke, R., Fink-Jensen, A., Jessop, D. S., Moller, M., and Sheikh, S. P. (1996) *Am. J. Physiol.* **271,** R848–R856
37. White, R. B., Broqua, P., Meyer, J., Junien, J.-L., and Aubert, M. L. (2000) *82nd Annual Meeting of the Endocrine Society*, June 21–24, *Toronto, Ontario, Canada*, p. 271, Abstr. 1115, The Endocrine Society Press, Bethesda, MD
38. Chomczynski, P., and Sacchi, N. (1987) *Anal. Biochem.* **162,** 156–159
39. Piechaczyk, M., Blanchard, J. M., Marty, L., Dani, C., Panabieres, F., El Sabouty, S., Fort, P., and Jeanteur, P. (1984) *Nucleic Acids Res.* **12,** 6951–6963
40. Drucker, D. J., Shi, Q., Crivici, A., Sumner-Smith, M., Tavares, W., Hill, M., Deforest, L., Cooper, S., and Brubaker, P. L. (1997) *Nat. Biotechnol.* **15,** 673–677
41. DaCambra, M. P., Yusta, B., Sumner-Smith, M., Crivici, A., Drucker, D. J., and Brubaker, P. L. (2000) *Biochemistry* **39,** 8888–8894
42. Yusta, B., Somwar, R., Wang, F., Munroe, D., Grinstein, S., Klip, A., and Drucker, D. J. (1999) *J. Biol. Chem.* **274,** 30459–30467
43. Scrocchi, L. A., Brown, T. J., MacLusky, N., Brubaker, P. L., Auerbach, A. B., Joyner, A. L., and Drucker, D. J. (1996) *Nat. Med.* **2,** 1254–1258
44. Sherwood, N. M., Krueckl, S. L., and McRory, J. E. (2000) *Endocr. Rev.* **21,** 619–670
45. Lankat-Buttgereit, B., and Goke, B. (1997) *Peptides (Elmsford)* **18,** 617–624
46. Galehshahi, F. S., Goke, B., and Lankat-Buttgereit, B. (1998) *FEBS Lett.* **436,** 163–168
47. Wildhage, I., Trusheim, H., Goke, B., and Lankat-Buttgereit, B. (1999) *Endocrinology* **140,** 624–631
48. Portois, L., Maget, B., Tastenoy, M., Perret, J., and Svoboda, M. (1999) *J. Biol. Chem.* **274,** 8181–8190
49. Gutzwiller, J. P., Drewe, J., Goke, B., Schmidt, H., Rohrer, B., Lareida, J., and Beglinger, C. (1999) *Am. J. Physiol.* **276,** R1541–R1544
50. Meeran, K., O'Shea, D., Edwards, C. M., Turton, M. D., Heath, M. M., Gunn, I., Abusnana, S., Rossi, M., Small, C. J., Goldstone, A. P., Taylor, G. M., Sunter, D., Steere, J., Choi, S. J., Ghatei, M. A., and Bloom, S. R. (1999) *Endocrinology* **140,** 244–250
51. Scrocchi, L. A., and Drucker, D. J. (1998) *Endocrinology* **139,** 3127–3132
52. Donahey, J. C. K., van Dijk, G., Woods, S. C., and Seeley, R. J. (1998) *Brain Res.* **779,** 75–83
53. Thiele, T. E., van Dijk, G., Campfield, L. A., Smith, F. J., Burn, P., Woods, S. C., Bernstein, H., and Seeley, R. J. (1997) *Am. J. Physiol.* **272,** R726–R730
54. Thiele, T. E., Seeley, R. J., D'Alessio, D., Eng, J., Bernstein, I. L., Woods, S. C., and van Dijk, G. (1998) *Brain Res.* **801,** 164–170
55. Rinaman, L. (1999) *Am. J. Physiol.* **277,** R1537–R1540
56. Goke, R., Fehmann, H.-C., Linn, T., Schmidt, H., Krause, M., Eng, J., and Gŝke, B. (1993) *J. Biol. Chem.* **268,** 19650–19655
57. Alvarez, E., Roncero, I., Chowen, J. A., Thorens, B., and Blazquez, E. (1996) *J. Neurochem.* **66,** 920–927
58. Sivarajah, P., Wheeler, M. B., and Irwin, D. M. (2001) *Comp. Biochem. Physiol.* **128,** 517–527
59. Traber, P. G., and Silberg, D. G. (1996) *Annu. Rev. Physiol.* **58,** 275–297
60. Boylan, M. O., Jepeal, L. I., Jarboe, L. A., and Wolfe, M. M. (1997) *J. Biol. Chem.* **272,** 17438–17443
61. Dusing, M. R., Brickner, A. G., Lowe, S. Y., Cohen, M. B., and Wiginton, D. A. (2000) *Am. J. Physiol.* **279,** G1080–G1093
62. Jin, T., and Drucker, D. J. (1996) *Mol. Cell. Biol.* **16,** 19–28
63. Larsen, P. J., Tang-Christensen, M., and Jessop, D. S. (1997) *Endocrinology* **138,** 4445–4455
64. MacLusky, N., Cook, S., Scrocchi, L., Shin, J., Kim, J., Vaccarino, F., Asa, S. L., and Drucker, D. J. (2000) *Endocrinology* **141,** 752–762
65. Oka, J., Suzuki, E., and Kondo, Y. (2000) *Brain Res.* **878,** 194–198
66. van Dijk, G., and Thiele, T. E. (1999) *Neuropeptides* **33,** 406–414
67. Franklin, K., and Paxinos, G. (1997) *The Mouse Brain in Sterotaxic Coordinates*, Academic Press, Inc., San Diego, CA